Open access • Journal Article • DOI:10.1039/C8TA02288G

Recent progress in 2D/quasi-2D layered metal halide perovskites for solar cells

Jielin Yan, Jielin Yan, Weiming Qiu, Weiming Qiu ...+4 more authors

Institutions: IMEC, Zhejiang University, Katholieke Universiteit Leuven

Published on: 19 Jun 2018 - Journal of Materials Chemistry (The Royal Society of Chemistry)

Topics: Perovskite (structure)

Journal Name

ARTICLE

Recent progress on 2D/quasi-2D layered metal halide perovskites for solar cells

Jielin Yan[a,b], Weiming Qiu[b*], Gang Wu[a], Paul Heremans[b], Hongzheng Chen[a*]

Received 00th January 20xx,
Accepted 00th January 20xx

DOI: 10.1039/x0xx00000x

www.rsc.org/

As an important category of perovskite materials, two-dimensional (2D) perovskites are attracting increasing research attention these days. Their possibility of combining high performance and stability for perovskite based optoelectronic devices has triggered a new wave of research. This review mainly focuses on the application of 2D perovskite materials for solar cells. We start with a brief introduction of 2D perovskite structure and its unique properties. The recent progress in 2D perovskite solar cells is summarized in three aspects according to the existing forms of the perovskite materials in the devices. In the end, a short outlook with our opinion is given to indicate the possible development trend for this kind of perovskite materials.

Introduction

Metal halide perovskite materials have shown plenty of outstanding optoelectronic properties, such as strong light harvesting capability, long charge carrier diffusion length,[1] high defect tolerance,[2] large mobilities,[3] and very narrow photoluminescence with high quantum yield,[4] etc. These unique properties make them star materials for applications like solar cells, light emitting diodes (LEDs), lasers, photodetectors and so on and thus have been widely studied recently. Especially, since the first report of perovskite solar cells by Miyasaka in 2009,[5] this new class of thin-film solar cells have gone through an unprecedented rapid development.[6-11] So far, the certified power conversion efficiency (PCE) of small-area (< 1cm^2) perovskite solar cells has reached 22.7% in lab, and significant progress has also been made in field of large-area perovskite modules.[10-15] However, on the downside, the instability of perovskite solar cells over moisture, light and heat[16-18] remains as the main stumbling block towards the commercialization of this technology.

Lots of efforts have been done to enhance the stability of devices made from perovskite materials, including compositional engineering,[15, 19, 20] interface engineering,[21-26] encapsulation technique,[27] device structure engineering.[28, 29] Among these, one of the promising strategies is to lower the dimension of perovskites from three-dimension (3D) to two-dimension (2D) which presents higher stability against ambient.[30, 31] Recently, these kinds of layered 2D perovskites have been demonstrated to exhibit over 13% PCE in solar cells with better stability, compared to its 3D counterparts.[32] Nevertheless, the layered structure may also bring some unfavourable characteristics. First, the undesired orientation of the layer structure can cause charge transport problems inducing charge accumulation and more recombination loss.[33, 34] Second, bandgap increases when reducing the dimension of perovskite, leading to further deviation from ideal bandgap for single junction solar cells. Both of mentioned above can degrade the efficiency of perovskite solar cells. Therefore, it is of significant importance to control the orientation and the dimension of the layered perovskite to achieve the optimal balance of stability and efficiency, which has already trigged enormous research interest these days.

In this review, we highlight recent advances of 2D layered perovskites for photovoltaics. First, we will present a detailed discussion of 2D layered perovskites' structure and their unique properties. Second, the photovoltaic applications of 2D layered perovskites are divided into three parts according to their existing forms in devices and discussed respectively. Finally, we will give a summary and outline the perspectives toward high-performance 2D layered perovskite solar cells

1. 2D layered perovskite: structure and unique properties

In 1957, Ruddlesden and Popper first reported A_2BO_4 typed compounds which have a similar crystal structure with today's 2D layered perovskite and that is how the name of Ruddlesden-Popper perovskite came.[35] The general formula of such Ruddlesden-Propper layered perovskite is $(RNH_3)A_{n-1}B_nX_{3n+1}$ (n = 1, 2, 3, 4……) (**Figure 1**a), where $(A_{n-1}B_nX_{3n+1})^{2-}$ denotes the conductor layer derived from the parent 3D perovskite, such as methylammonium (MA) lead iodide ($MAPbI_3$), formamidinium (FA) lead iodide ($FAPbI_3$), cesium (Cs) lead iodide ($CsPbI_3$). The conductor layers are isolated from one another by means of R-NH_3, the large aliphatic or aromatic alkylammonium spacer cation such as phenylethylammonium (PEA), butylammonium

[a] State Key Laboratory of Silicon Materials, MOE Key Laboratory of Macromolecular Synthesis and Functionalization, Department of Polymer Science and Engineering, Zhejiang University, Hangzhou 310027, P. R. China.
[b] IMEC, Kapeldreef 75, Heverlee, B-3001, Belgium.

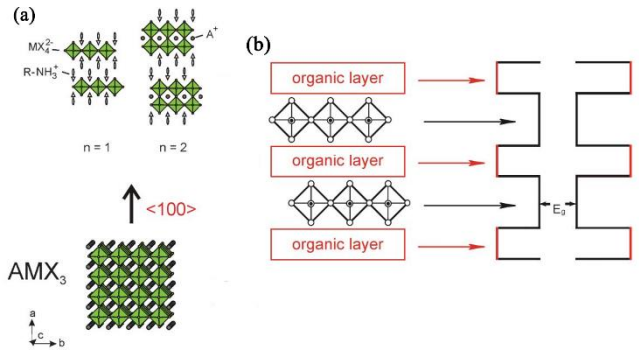

Figure 1. a) The crystalline structures of layered perovskites derived from the basic 3D AMX_3 structure by taking cuts from along <100> crystallographic direction. R is an organic moiety, A is a small organic cation (or monovalent inorganic cation), M is generally a divalent metal and X is a halide. The metal halide octahedral units, MX_6, are shown schematically in polyhedral representation. b) Schematic organic-inorganic perovskite structure and the most common resulting energy level arrangement. Inorganic slabs alternate with organic layers having much wider bandgap, resulting in a quantum well structure.[36] Adapted with permission from Ref. 36. Copyright 2004 The Royal Society of Chemistry.

(BA). The thickness, which is decided by the n value in the formula, of each conductor layer can be adjusted by careful control of the stoichiometry.

The insertion of insulating spacer cation brings 2D layered perovskite unique properties compare to 3D counterparts. First, the hydrophobic nature of organic spacer imparts 2D perovskites with superior moisture stability. For instance, the reactions between water and $MAPbI_3$ can be generally explained by a series of equilibria within the PbI_2-MAI-H_2O system as described by Equations (1)–(4).[37] While the existence of organic spacer layers slows down this reaction at second step by isolating 3D perovskite slabs from water molecules.[37]

$$PbI_2 + MAI \Leftrightarrow MAPbI_3 \quad (1)$$

$$MAPbI_3 + H_2O \Leftrightarrow MAPbI_3 \cdot H_2O \quad (2)$$

$$(4\text{-}n)\ MAPbI_3 + n\ MAPbI_3 \cdot H_2O + (2\text{-}n)\ H_2O \Leftrightarrow (MA)_4PbI_6 \cdot 2H_2O + 3PbI_2 \quad (3)$$

$$(MA)_4PbI_6 \cdot 2H_2O \Leftrightarrow PbI_2 + 4MAI + 2H_2O \quad (4)$$

Second, the electrical insulation nature of organic spacer and almost unchanged conductivity of perovskite conductor layers give rise to the natural multiple-quantum-well structure as shown in Figure 1b: the perovskite layers serve as the potential "well" while the organic spacer layers play the role of the potential "wall".[38] Excitons are formed instead of free holes and electrons when 2D layered perovskites are excited because of increased binding energy by such quantum confinement effect.[39] Furthermore, the transient photoconductivity experiments by time-resolved terahertz spectroscopies verified that charges prefer transporting along the lead iodide planes, i.e. the so-called "well".[40] As the inorganic layer thickness decreases, the quantum confinement effect comes prominence. As a result, exciton absorption and shark emission peaks can be observed and blue-shifted when n decreases (**Figure 2**a-c). In reality, it is hard to get phase-pure (perovskite crystals with the same n value) 2D layered perovskite films, and in literatures the n values are often calculated from the composition in the precursor solutions. This is widely convinced by multiple exciton response peaks in absorption and photoluminescence (PL) spectra (Figure 2d-e).[41, 42] Due to this fact, the charge carrier dynamics is much more complicated in 2D perovskite films than in the 3D ones. It is worthy to mention that such multiple-quantum-well structure is favourable to light emitting diode devices. The lower bandgap regions that generate electroluminescence can effectively confined by perovskite quantum wells with higher energy gaps, resulting in very efficient radiative recombination that leads to perovskite light emitting diode with high external quantum efficiency over 10%.[42-44] On the other hand, such unique structure of 2D layered perovskites also makes the charge transport in their films anisotropic and highly dependant on the orientation of the layered structure.[40] The charge mobility is much higher in the direction along the perovskite slabs than in the direction perpendicular to the orientation of these slabs. Thus, for solar cells, it is important to have the perovskite slabs with the out-of-plane orientation, such that thicker films with balanced charge transport and light absorption can be used to achieve a high PCE.

Third, the structure of 2D perovskites can be easily tuned not only by tuning the composition of perovskite layers but also by molecular design of the spacer cations, such as alkyl chain length,[45] ammonium dications,[46] insertion of π-conjugated segment.[47] Thus, a much wider range of optoelectronic properties can be tuned for 2D perovskites than for 3D perovskites. The versatility in designing the compositions and thus optoelectronic properties of 2D layer perovskite gives them the opportunity to be used in an even more broad range of applications, compared to 3D perovskites.[48] Besides the most used PEA and BA, iso-butylammonium (iso-BA),[49] iodoethylammonium ($IC_2H_4NH_3$),[50] ethylenediammonium (EDA),[46] ammoniumvaleric acid (AVA),[51, 52] cyclopropylammonium (CA),[53] polyethylenimine (PEI),[54] benzylammonium (BA*),[55, 56] octylammonium (OA)[57] etc. have also been reported as spacer cations.

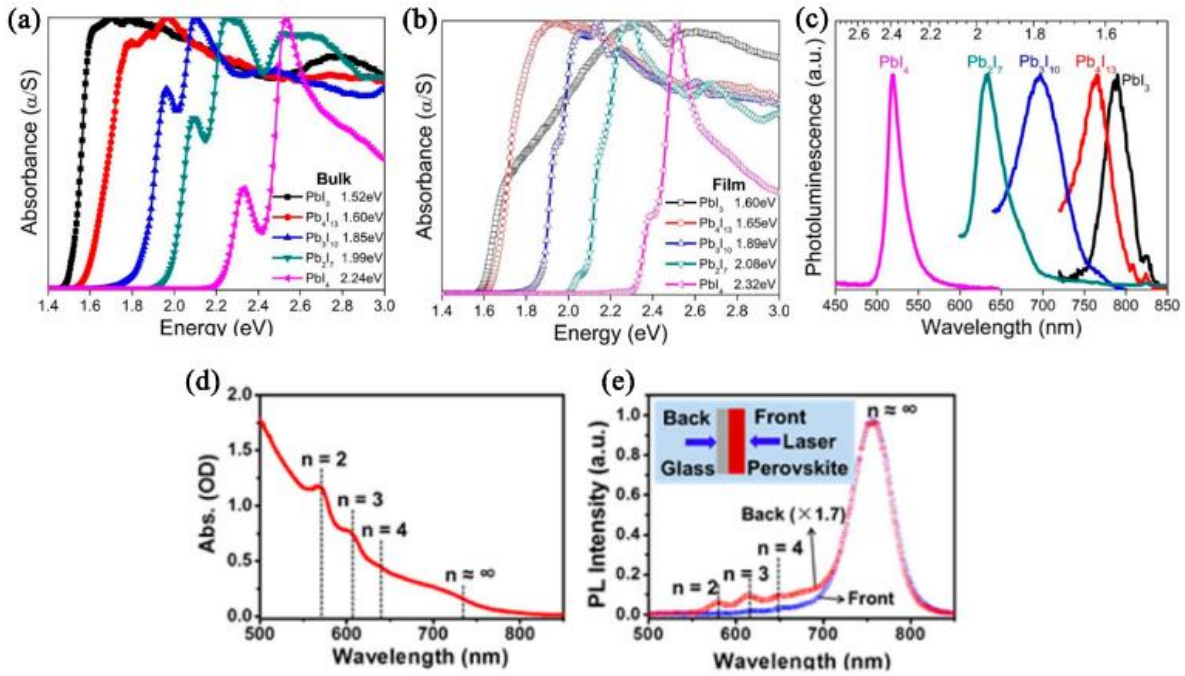

Figure 2. Optical band gaps of (a) bulk, (b) spin-coated TiO_2-perovskite thin films, and (c) PL spectra of spin-coated glass-perovskite thin films of the $MAPbI_3$ and $(BA)_2(MA)_{n-1}Pb_nI_{3n+1}$ compounds. Reproduced with permission from Ref. 31. Copyright 2015 American Chemical Society. (d) UV–vis absorption spectrum of a typical $(BA)_2(MA)_{n-1}Pb_nI_{3n+1}$ 2D perovskite film (~358 nm thickness, prepared as n = 4). The perovskite film exhibited multiple absorption peaks, which are identified as n = 2 (2.17 eV), n = 3 (2.04 eV), n = 4 (1.93 eV) and n ≈ ∞ perovskite phases. (e) Comparison of the emission spectra of the 2D perovskite film illuminated from the front and back sides (as illustrated in the inset) of the film. Under back-excitation, the spectrum shows emission peaks from n = 2, 3 and 4 phases in addition to the dominant emission from n ≈ ∞ phase. Reproduced with permission from Ref. 41. Copyright 2017 American Chemical Society

There are many other interesting properties that make 2D layered perovskite materials attractive, and probably even more to be explored in future. For example, ion migration has been an issue for perovskite solar cells using 3D perovskites, while Huang and co-workers recently reported that the activation energy of ion migration in 2D perovskites was significantly higher than that in 3D perovskites with similar compositions.[58] Crochet and Mohite *et al.* unveiled an "edge states" that existed in the perovskite layers when n > 2. These states provide a direct pathway for dissociating excitons into longer-lived free carriers that substantially improve the performance of optoelectronic devices.[59]

2. 2D layered perovskites for photovoltaics

Taking the advantage of easily tuning their properties through chemistry and quantum mechanics, as well as their high environmental stability, 2D layered perovskites have already played an important role in perovskite photovoltaics. Herein we discuss the progress of 2D layered perovskites for photovoltaics in three aspects, according to their main functions in perovskite solar cells. The performance and device structures of 2D perovskite solar cells reported so far are summarized in **Table 1.**

Table 1. Summary of 2D perovskite structures and their solar cell performances. Note: 'PVK' represents "perovskite".

	Spacer Cation	Perovskite	Device structure	V_{oc} [V]	J_{sc} [mA cm^{-2}]	FF	PCE [%]
2D as absorber	PEA	$(PEA)_2(MA)_2Pb_3I_{10}$	FTO/c-TiO_2/PVK/spiro-OMeTAD/Au	1.18	6.72	0.60	4.73[30]
		$(PEA)_2(FA)_8Sn_9I_{28}$	ITO/NiO_x/PVK/PCBM/Ag	0.59	14.44	0.69	5.94[58]
		$(PEA)_2(MA)_4Pb_5I_{16}$	ITO/PEDOT:PSS/PVK/PCBM/BCP/Ag	1.11	15.01	0.67	11.01[60]
	BA	$(BA)_2(MA)_2Pb_3I_{10}$	FTO/c-TiO_2/m-TiO_2/PVK/spiro-OMeTAD/Au	0.93	9.42	0.46	4.02[31]
		$(BA)_2(MA)_3Pb_4I_{13}$	ITO/PEDOT:PSS/PVK /PCBM/Al	1.01	16.76	0.74	12.51[61]
		$(BA)_2[Cs_{0.05}(MA)_{0.95}]_3Pb_4I_{13}$	FTO/c-TiO_2/PVK/spiro-OMeTAD/Au	1.08	19.95	0.63	13.68[32]

	Spacer Cation	Perovskite	Device structure	V_{oc} [V]	J_{sc} [mA cm^{-2}]	FF	PCE [%]
		$(BA)_2CsPb_2I_7$	FTO/c-TiO_2/PVK/spiro-OMeTAD/Au	0.95	8.88	0.57	4.84[62]
		$(BA)_2(MA)_2Sn_3I_{10}$	FTO/c-TiO_2/m-TiO_2/PVK/PTAA/Au	0.38	8.9	0.57	1.94[63]
		$(BA)_2(MA)_3Sn_4I_{13}$		0.23	24.1	0.46	2.53[63]
		$(BA)_2(MA)_4Pb_5I_{16}$	ITO/PEDOT:PSS/PVK /PCBM/Al	0.98	15.5	0.65	10.0[64]
		$(BA)_2(MA)_2Pb_3I_{10}$	ITO/PEDOT:PSS/PVK /PCBM/BCP/Ag	0.97	12.79	0.55	6.89[34]
		$(BA)_2(MA)_3Pb_4I_{13}$	ITO/PEDOT:PSS/PVK /PCBM/BCP/Ag	0.98	14.71	0.61	8.79[34]
		$(BA)_2(FA)_2Pb_3I_{10}$	ITO/PE-DOT:PSS/PVK/PCBM/BCP/Ag	0.98	11.89	0.59	6.88[65]
		$(BA)_2(MA_{0.8}FA_{0.2})_3Pb_4I_{13}$	ITO/PEDOT:PSS/PVK /PCBM/BCP/Ag	0.99	18.12	0.71	12.81[66]
	Iso-BA	(iso-BA)$_2$(MA)$_3$Pb$_4$I$_{13}$ (RT)	ITO/C_{60}/PVK/spiro-OMeTAD/Au	1.14	14.87	0.52	8.82[49]
		(iso-BA)$_2$(MA)$_3$Pb$_4$I$_{13}$ (HC)		1.20	16.54	0.54	10.63[49]
2D-3D mixed	$IC_2H_4NH_3$	$(IC_2H_4NH_3)_2[(MA)_{1-y}(FA)_y]_{n-1}Pb_nI_{3n+1}$	FTO/c-TiO_2/m-TiO_2/PVK/spiro-OMeTAD/Au	0.88	14.88	0.69	9.03[50]
	BA	$(BA)_{0.05}(FA_{0.83}Cs_{0.17})_{0.95}Pb(I_{0.8}Br_{0.2})_3$	FTO/SnO_2/PC_{61}BM/PVK/spiro-OMeTAD/Au	1.14	22.7	0.80	20.6[67]
		$(BA)_{0.05}(FA_{0.83}Cs_{0.17})_{0.95}Pb(I_{0.6}Br_{0.4})_3$	FTO/SnO_2/PC_{61}BM/PVK/spiro-OMeTAD/Au	1.18	19.8	0.73	17.2[67]
	EDA	$CsPbI_3 \cdot 0.025EDAPbI_4$	FTO/c-TiO_2/PVK/spiro-OMeTAD/Ag	1.15	14.53	0.71	11.86[46]
	PEA	$FA_xPEA_{1-x}PbI_3$	ITO/NiO_x/PVK/PCBM/bis-C_{60}/Ag	1.04	22.08	0.77	17.71[68]
		$PEA_2MA_{n-1}Pb_nBr_{3n+1}$	FTO/TiO_2/PVK/spiro-OMeTAD/Au	1.46	9.0	0.65	8.5[69]
2D as interfacial layer	PEA	$MAPbI_3/(PEA)_2Pb_2I_4$	FTO/NiO_x/PVK/PCBM(PN4N)/Ag	1.17	21.80	0.78	19.89[70]
		$PEA_2SnI_4/FASnI_3$	ITO/PE-DOT:PSS/PVK/C_{60}/BCP/Al	0.53	24.1	0.71	9.0[71]
	AVA	$(AVA)_2PbI_4/MAPbI_3$	FTO/c-TiO_2/m-TiO_2/PVK/spiro-OMeTAD/Au	1.02	18.84	0.75	14.60[52]
		$(AVA)_2PbI_4/MAPbI_3$	FTO/c-TiO_2/m-TiO_2/ZrO_2:PVK/carbon	0.84	23.99	0.63	12.71[52]
		$(FAPbI_3)_{0.88}(CsPbBr_3)_{0.12}/(AVA)_2PbI_4$	FTO/c-TiO_2/m-TiO_2/PVK/CuSCN/Au	1.06	21.93	0.72	16.75[51]
	CA	$MAPbI_xCl_{3-x}/CA_2PbI_4$	ITO/PE-DOT:PSS/PVK/PCBM/rhodamine 101/LiF/Ag	0.92	19.29	0.77	13.86[53]
	PEI	$(PEI)_2PbI_4/MAPbI_xCl_{3-x}$	ITO/PE-DOT:PSS/PVK/PCBM/LiF/Ag	1.07	19.0	0.68	13.8[54]
	BA*	$(BA^*)_2PbI_4/Cs_{0.15}FA_{0.85}Pb(I_{0.73}Br_{0.27})_3$	FTO/c-TiO_2/PVK/spiro-OMeTAD/Au	1.24	19.83	0.73	18.13[55]
	OA	N/A	FTO/c-TiO_2/m-TiO_2/PVK/spiro-OMeTAD/Au	1.02	19.37	0.76	15.19[57]

2.1 2D layered perovskites with low n value as light absorber

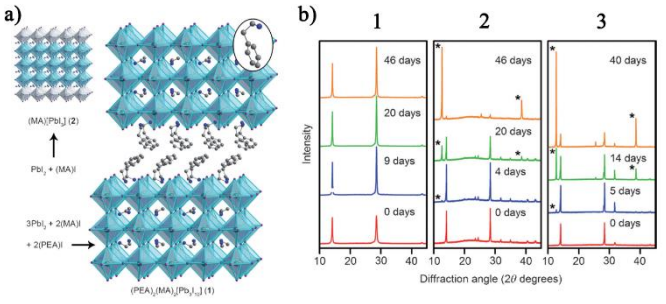

Figure 3. a) Crystal structures of the 3D perovskite (MA)(PbI_3) (2) and the 2D perovskite $(PEA)_2(MA)_2(Pb_3I_{10})$ (1). b) Powder XRD patterns of films of $(PEA)_2(MA)_2(Pb_3I_{10})$ (1), (MA)(PbI_3) formed from PbI_2 (2), and (MA)(PbI_3) formed from $PbCl_2$ (3), which were exposed to 52% relative humidity. Reproduced with permission from Ref. 30. Copyright 2014, Wiley-VCH.

Nurmikko and co-workers first synthesized $(PEA)_2(MA)_{n-1}Pb_nI_{3n+1}$ 2D layered perovskite in 1992, and their electrical properties were carefully studied.[38] However, until 2014 Karunadasa and co-workers demonstrated the first usage of such 2D layered perovskite (**Figure 3**a) in the planar solar cells as the light absorber, yielding a PEC of 4.73%.[30] A large V_{oc} of 1.18 V was achieved because of the increased bandgap of 2.1 eV. Moreover, as shown in Figure 3b, the layered 2D perovskite demonstrates excellent stability against moisture with almost unchanged X-ray diffraction (XRD) patterns after 46 days storage at a relative humidity of 52%. Later, by replacing PEA with non-aromatic spacer cation BA, Kanatzidis and co-workers reported $(BA)_2(MA)_{n-1}Pb_nI_{3n+1}$ perovskite solar cells with a similar PCE of 4.02%.[31] They found that the bandgap increased from 1.52 eV to 2.24 eV when n decreased from n = ∞ to n = 1 for BA-based perovskites. This trend is the same for PEA-based 2D perovskites. However, the BA-based 2D perovskites always show smaller bandgap than the PEA-based ones when the n value is the same, indicating the large cations do play a role in determining the perovskite film properties.

Although the device stability was significantly improved in the above-mentioned two cases, the reported PCEs were far from satisfactory. In order to achieve good perovskite solar cell performance in terms of both PCE and stability, two main factors need to be taken into consideration. First, suitable n values are required for 2D perovskites. On one hand, n should be large enough so that adequate light absorption and efficient charge extraction can be reached, on the other hand, it also should be small enough to fully keep the 2D layered nature. Second, the 2D crystals should have well out-of-plane orientation to facilitate the charge transport towards electrodes. While the n values can be largely controlled by tuning the composition of precursor solutions, the growth of those 2D perovskites with different n values shows quite different thermodynamic behaviours. For example, Kanatzidis *et al*. have shown the growth of $(BA)_2(MA)_{n-1}Pb_nI_{3n+1}$ tended to vary from in-plane orientation, random orientation and out-of-plane orientation, with the increase of n from 1 to 4 (see **Figure 4**).[31] Besides, as the n value increases, the differences in thermodynamic stability of the higher n-members become progressively smaller, it becomes difficult to get phase-pure 2D perovskites with n > 4.[64] Therefore, in order to get better control on the growth orientation and purity of 2D perovskites, new synthetic strategies are required.[47]

One of the biggest breakthroughs in making highly efficient and stable 2D perovskite solar cells was done by Mohite and co-workers together with Kanatzidis and co-workers, who introduced a hot-cast method for perovskite film formation.[61] The hot-cast technique resulted in near single-crystalline films, in which the crystal grains had a strongly out-of-plane preferential alignment (**Figure 5**a-c). This significantly improved the charge transport from the perovskite films to the electrodes, leading to significant PCE improvement from 4.02% to 12.52%. Moreover, the authors used 2D perovskite single crystals to prepare the precursor solutions, ensuring clean perovskite film formation with the desired composition, as has also been reported in another work.[63] Besides the high PCE, the unencapsulated devices in

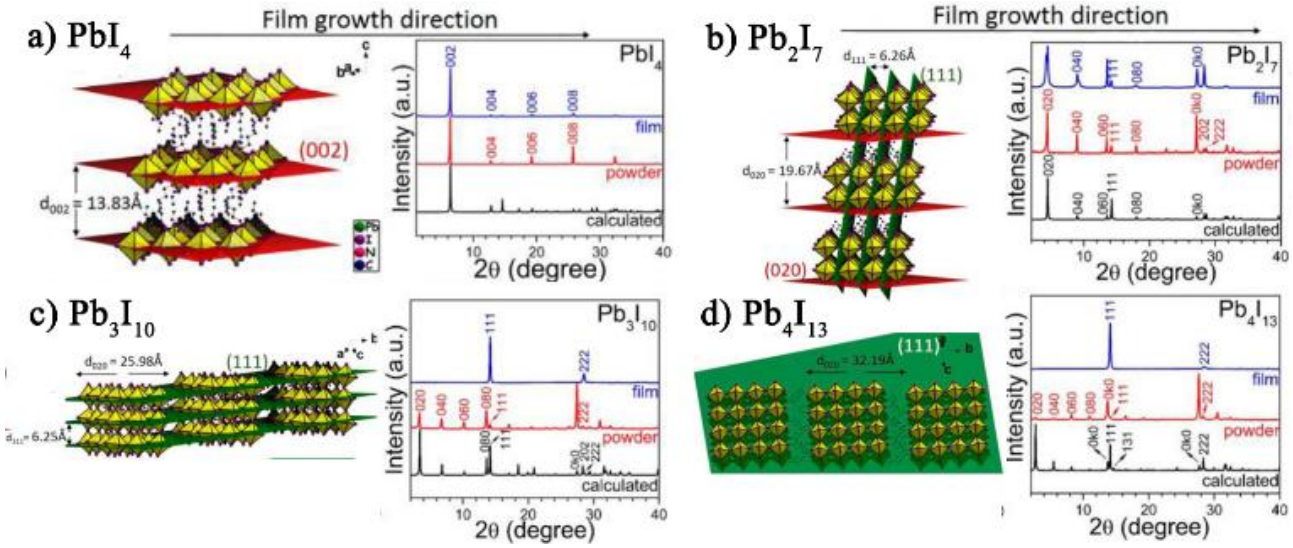

Figure 4. XRD patterns of thin films vs bulk materials of (a) BA_2PbI_4 perovskites, (b) $(BA)_2(MA)Pb_2I_7$, (c) $(BA)_2(MA)_2Pb_3I_{10}$, and (d) $(BA)_2(MA)_3Pb_4I_{13}$ perovskites, with the illustration of their respective diffraction planes. Reproduced with permission from Ref. 31. Copyright 2015 American Chemical Society.

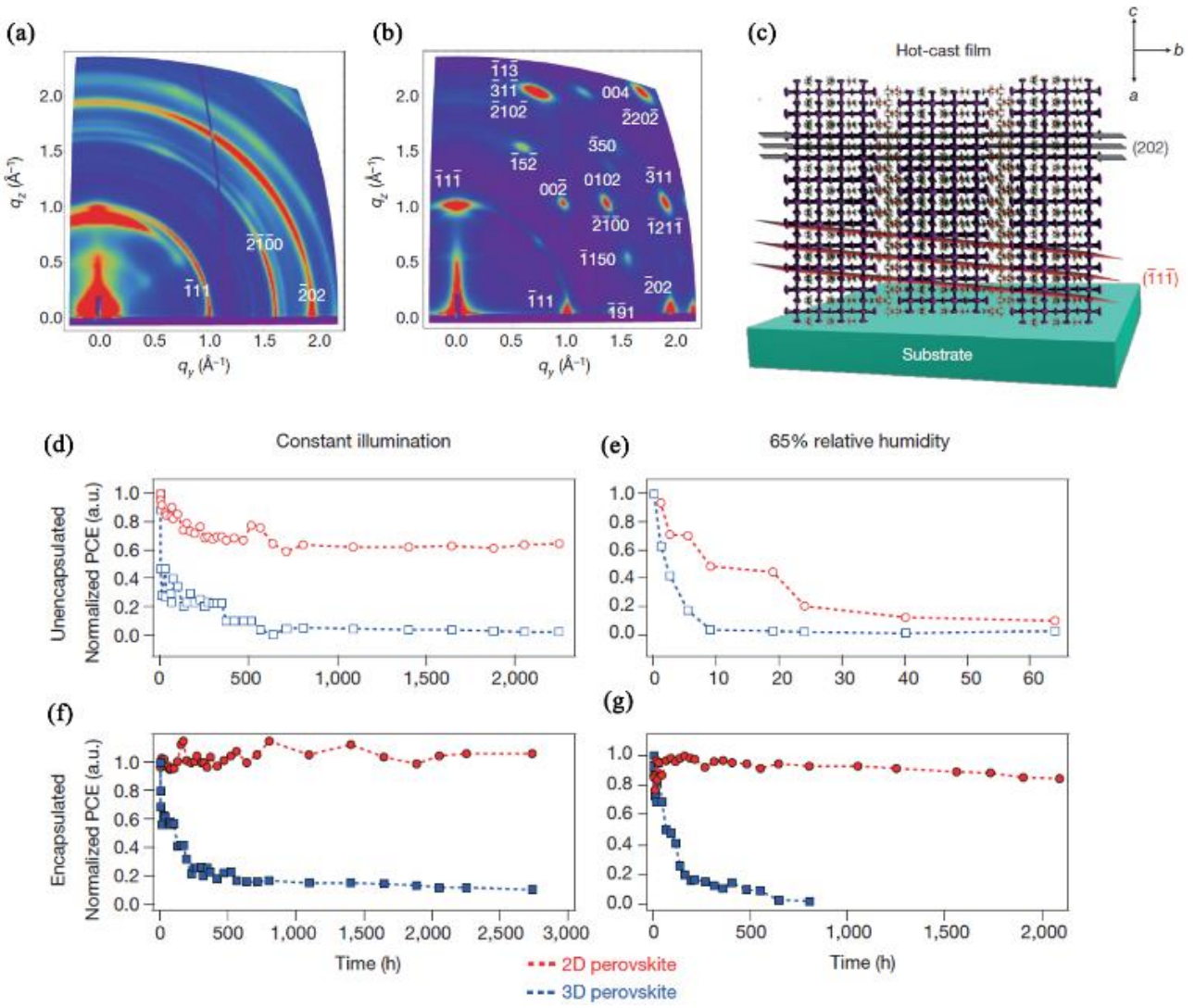

Figure 5. Grazing incidence wide-angle X-ray scattering (GIWAXS) maps for room-temperature-cast polycrystalline (a) and hot-cast near single-crystalline (b) $(BA)_2(MA)_3Pb_4I_{13}$ perovskite films. c) Schematic representation of the (101) orientation, along with the (111) and (202) planes of a 2D perovskite crystal, consistent with the GIWAXS data. Photostability tests under constant AM1.5G illumination for 2D ($(BA)_2(MA)_3Pb_4I_{13}$; red) and 3D ($MAPbI_3$; blue) perovskite devices without (d) and with (f) encapsulation. Humidity stability tests under 65% relative humidity in a humidity chamber for 2D ($(BA)_2(MA)_3Pb_4I_{13}$; red) and 3D ($MAPbI_3$; blue) perovskite devices without (e) and with (g) encapsulation. Reproduced with permission from Ref. 61. Copyright 2016, Nature Publishing Group.

this work also exhibited slower degradation under constant light illumination or high relative humidity (65% RH) than the 3D counterparts (Figure 5d-g). This is due to the long and bulkier hydrophobic organic side groups in the 2D perovskite structure that can protect them from moisture. By borrowing this hot-cast method, Liu and co-workers prepared Cs-doped 2D $(BA)_2(MA)_3Pb_4I_{13}$ perovskite solar cells with the highest reported PCE of 13.7%, using low n (n = 4) 2D perovskites. Doping Cs cations into 2D $(BA)_2(MA)_3Pb_4I_{13}$ perovskites was found to help increase the grain size, reduce the trap-state density, improve the charge carrier mobility and charge transfer kinetics, and thus lead superior PCE.[32]

In addition, Kanatzidis *et al*. further modified the hot-casting method to make it suitable for the preparation of high-quality 2D layered perovskite films with relative high n values.[64] By engineering the solvent in the precursor solutions for the hot-casting process, more specifically, by varying the ratio of dimethylsulfoxide (DMSO) and N,N-dimethylformamide (DMF), they yielded highly out-of-plane oriented perovskite films with n = 5. They found, without the use of DMSO, the extremely rapid solvent evaporation during the hot-casting process led to imperfect self-assembly of perovskite slabs and hence low crystallinity films. On the contrary, the adding of DMSO, which has a high affinity for the metal halide, can result in the formation of an intermediate solvated phase that retards the crystallization rate.[64, 72] Planar heterojunction solar cell devices incorporating these hot-casting n = 5 films from optimized 3:1 DMF:DMSO solvent mixtures yield an impressive PCE of 10%.

Although the hot-casting method is very effective to make high-quality well-oriented 2D perovskite films, the drawbacks are that it will be difficult to precisely control the substrate temperature during spin-coating, and it may not be easy to scale up

for large-area fabrication. Therefore, it is highly required to develop more convenient methods to prepare 2D perovskite films with similar properties. So far, this was mainly done by precursor engineering. For example, Liang and co-workers reported that by replacing BA with shortly branched iso-BA as spacer cation,[49] the resulting (iso-BA)$_2$(MA)$_3$Pb$_4$I$_{13}$ exhibited a remarkable increase of orientation and crystallinity, even under the room-temperature (RT) cast condition. For comparison, the perovskite films based on linear BA only became oriented when hot casted. As a result, the highest PCE of 8.82% was obtained for RT casted (iso-BA)$_2$(MA)$_3$Pb$_4$I$_{13}$ based inverted bilayer solar cells. Furthermore, if the hot-casting method is applied to (iso-BA)$_2$(MA)$_3$Pb$_4$I$_{13}$, an even higher PCE of 10.63% was achieved. These (iso-BA)$_2$(MA)$_3$Pb$_4$I$_{13}$ films also shown superior ambient stability, maintaining its initial colour after 840 h storage without encapsulation in an environmental chamber at 20 °C and with a high RH of 60%. Zhou *et al*. found that the introduction of 20% FA to make ternary (BA)$_2$(MA, FA)$_3$Pb$_4$I$_{13}$ films could alter the crystal growth towards out-of-plane orientation, which resulted in devices with the best efficiency of 12.81%.[66]

Instead of changing the composition of the 2D perovskites, Chen *et al*. developed another precursor engineering route by applying additives to the precursor solutions. For example, vertically oriented 2D layered (BA)$_2$(MA)$_{n-1}$Pb$_n$I$_{3n+1}$ (n = 3, 4) perovskite films were fabricated with the aid of ammonium thiocyanate (SCN) additive through a one-step spin coating process.[34] The addition of SCN helped the formation of 2D perovskite films with reduced grain boundaries and also better out-of-plane orientation. Perovskite solar cells with a structure of ITO/PEDOT:PSS/(BA)$_2$(MA)$_2$Pb$_3$I$_{10}$/PC$_{61}$BM/BCP/Ag exhibited an averaged PCE of 6.82% (n = 3) and 8.79% (n = 4), with impressive shelf stability in ambient. Later, they further applied this additive controlled crystal growth method to prepare PEA based 2D layered perovskite with n = 5. Again, as shown by GIWAXS in **Figure 6**, the addition of SCN led to vertically-orientated highly-crystalline 2D perovskite films. As a result, the PCE of perovskite solar cells significantly increased from 0.56% to 11.01% when SCN was added into the precursor solution.[60] This PCE is also much higher than that of the device made with (BA)$_2$(MA)$_{n-1}$Pb$_n$I$_{3n+1}$ they reported earlier. The possible reason could be that, unlike the soft linear-chain spacer BA, the rigid benzene ring in PEA may confine the structural freedom to stabilize the oriented structure, and consequently facilitate the formation of highly crystalline 2D perovskite films with out-of-plane orientation even at a higher n value.[60] Inspired by this additive-assisted growth method, Chen *et al.* further found that thiourea could also be used to guide the out-of-plane growth of FA-based 2D perovskites. Impressively, they reported low bandgap FA-based 2D layered perovskite BA$_2$FA$_2$Pb$_3$I$_{11}$with Eg = 1.51 eV,[65] resulting in solar cells with a best PCE of 6.88% and neglectable hysteresis.

Besides the Pb-based perovskites, Sn-based 2D perovskites with low n values were also studied, and the lowering of the dimension had been shown to be beneficial for improving the stability of Sn-based perovskites. Recently Ning *et al.* realized highly orientated growth of low-dimensional (PEA)$_2$(FA)$_{n-1}$Sn$_n$I$_{3n+1}$ perovskite on nickel oxide (NiO$_x$) substrates, achieving a PCE up to 5.94%.[73] Their Sn-based 2D perovskites had significantly improved stability against oxidation. They claimed the reasons for this included threefolds: 1) the compact and smooth films protected the film from oxygen infiltration; 2) density functional theory (DFT) calculation demonstrated that the instability against the oxidation process was suppressed with decreasing n values; 3) the hydrophobic PEA cation also protect Sn^{2+} from oxygen. Due to the good air stability of 2D (PEA)$_2$(FA)$_{n-1}$Sn$_n$I$_{3n+1}$ films, their unencapsulated devices had no appreciable decay in efficiency after storing in glovebox over 100 h. In addition, Kanatzidis and co-workers reported (BA)$_2$(MA)$_{n-1}$Sn$_n$I$_{3n+1}$ based solar cells with a promising PCE of 2.5% for the n = 4 films.[63] The device maintains 90% of its initial performance after 1 month. In this case, they attributed the enhanced stability to the physical isolation of BA spacer cation and the usage of chemical antioxidant that suppressed the oxidation of Sn^{2+}

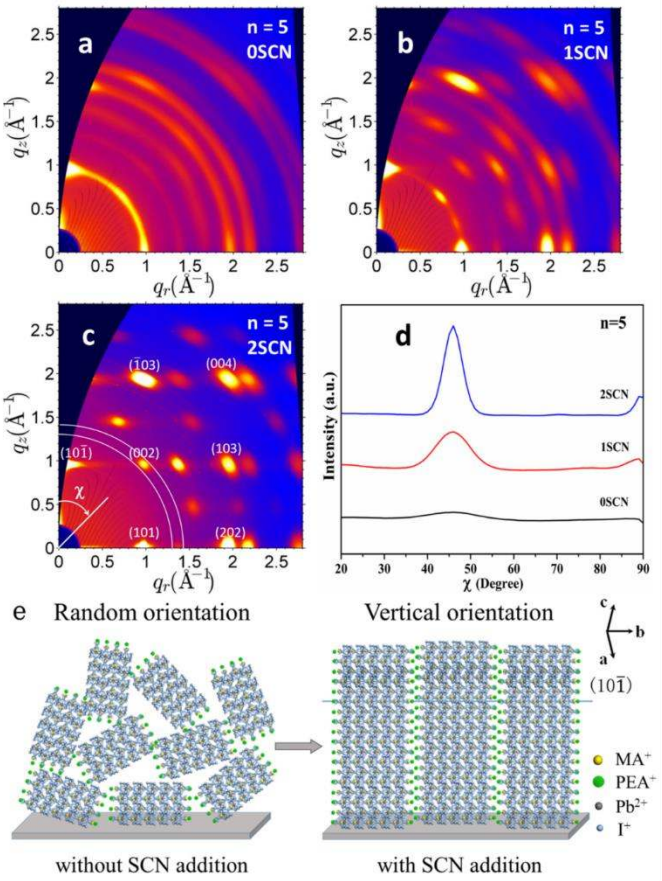

Figure 6. (a-c) 2D GIWAXS patterns of (PEA)$_2$(MA)$_4$Pb$_5$I$_{16}$ (n = 5) perovskite films with various addition amounts of NH$_4$SCN (a. 0SCN, b. 1SCN, c. 2SCN); (d) The polar intensity profiles along the ring in the q_r range of 1.30 to 1.42 Å^{-1}, as indicated in (c); (e) Schematic interpretation from random orientation to vertical orientation with SCN addition. Reproduced with permission from Ref. 60. Copyright 2018, Wiley-VCH.

2.2 2D-3D mixed perovskites as the light absorber

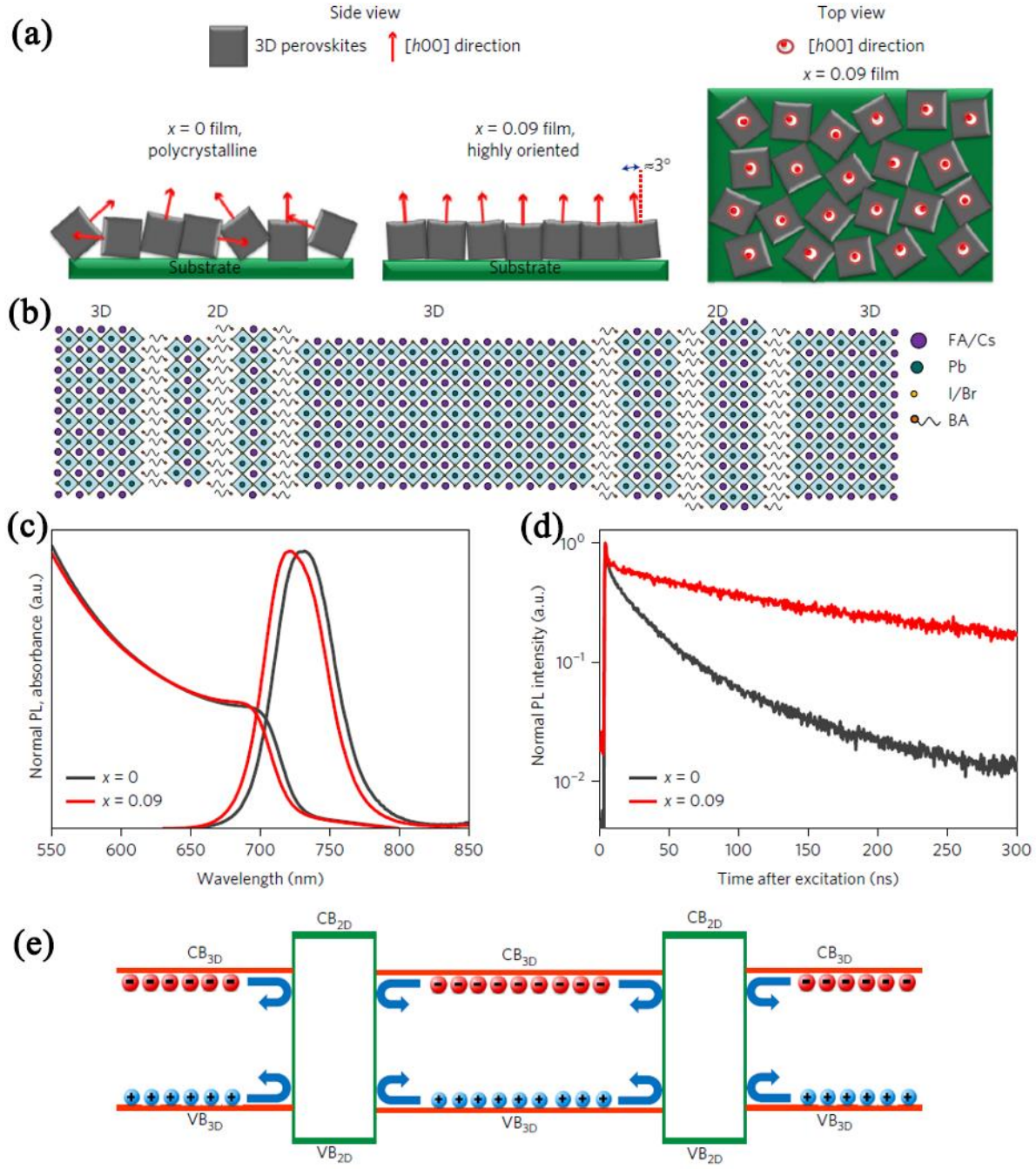

Figure 7. a) Illustration of the orientation of the 3D perovskite phase in the x = 0.09 film ($BA_x(FA_{0.83}Cs_{0.17})_{1-x}Pb(I_yBr_{1-y})_3$), compared with a low-textured x = 0 film, showing a preference for the [h00] direction to align out-of-plane and no preferential orientation within the plane. b) Schematic illustration of the proposed self-assembled 2D–3D perovskite film structure. c) Ultraviolet-visible absorption and PL spectra of an x = 0 film (black line) and an x = 0.09 film (red line). d) Time-resolved PL spectra for the same films. e) Proposed electronic band sets of the 2D–3D heterojunction. CB and VB stand for conduction band and valence band, respectively, with the subscript indicating either the 2D or 3D phase. Reproduced with permission from Ref. 67. Copyright 2017, Nature Publishing Group.

As the n value further increases, typically when n > 10, the properties of the resulting films are more like the corresponding 3D counterparts, yet one can still observe some features of 2D perovskites. In this case, the perovskite films are like a mixture of 2D and 3D perovskites. For example, Etgar and co-workers synthesized such quasi-2D mixed perovskites of $(PEA)_2(MA)_{n-1}Pb_nBr_{3n+1}$ (n = 20, 30, 40, 50, 60).[69] The absorption onset of these films with high n values closed to that of the 3D $MAPbBr_3$ film. But the 2D nature of these materials was supported by the observed reflection at 5.3° in the XRD pattern. The combination of 2D and 3D perovskites endowed their devices with ultrahigh V_{oc} of 1.46 V while unaffected PCE compared to 3D ones, indicating attractive candidates for tandem solar cells. They further studied the influence of spacer cation chain length on the properties of quasi-2D perovskites.[56] No obvious change was observed in the exciton binding energy and optical bandgap

by changing the spacer cations, i. e. benzyl ammonium, phenylethyl ammonium, and propylphenyl ammonium. However, the DFT and Spin-orbit coupling calculations did show the decrease in electrical conductivity of the perovskite films when the length of the organic spacer cations increased.

On the other hand, Snaith *et al.* found that by appropriately tuning the BA-to-FA/Cs ratio in $BA_x(FA_{0.83}Cs_{0.17})_{1-x}Pb(I_yBr_{1-y})_3$ perovskite films, plate-like 'layered' perovskite crystallites orientated perpendicularly to the plane of the film would form between the 3D perovskite grains. The plate-like 'layered' perovskite was demonstrated by XRD pattern to be 2D layered perovskite that formed due to the incorporation of BA cation in the precursor solutions. By virtue of the good lattice matching of 2D and 3D grains, the 3D perovskite grain growth was confined by the 2D grains, showing a high preference for the [100] direction to be aligned parallel to the film normal (**Figure 7**a). Besides, as shown in Figure 7b-e, since the bandgaps of 2D perovskite phases are wider than those of 3D phases, the electronic configuration allowed charges remaining in the 3D perovskite and not suffering from trapping and recombination at the grain boundaries, resulting in longer carrier lifetime. Their optimized devices showed average stabilized PCEs of 17.5 ± 1.3% and 15.8 ± 0.8% for perovskite films with bandgaps of 1.61 eV and 1.72 eV, respectively. Moreover, these devices could sustain 80% of the initial PCEs even after exposure to air for 1,000 h.[67]

Another advantage of 2D-3D mixed perovskites, which has been demonstrated by several groups, is to improve the stability of certain perovskite phases. For instance, Jen *et al.* reported that the phase stability of α-phase $FAPbI_3$ was greatly enhanced by mixing PEA cations into the film, making the $FA_xPEA_{1-x}PbI_3$ (n = 40) film stay unchanged after being kept in ambient for 30 days.[68] Zhao and co-workers introduced another bication, ethylenediamine cation (EDA^{2+}), to stabilize the α-phase $CsPbI_3$.[46] The terminal NH^{3+} groups on EDA^{2+} cations were expected to cross-link the α-$CsPbI_3$ perovskite crystal units, preventing the unwanted transition to the non-perovskite δ phase. The 2D-3D mixed films could retain their perovskite phase even after annealing at 100°C for a week, while the neat α-$CsPbI_3$ film transformed into a yellow δ-$CsPbI_3$ film within 12 h even at room temperature.

In addition, instead of adding 2D component to 3D perovskite bulk, Mathews *et al.* presented an inverse strategy to get 2D/3D mixed perovskites. A pure 2D perovskite (n = 1) was deposited first by spin coating the precursor solution containing a stoichiometric ratio of PbI_2 and iodoethylammonium iodide ($IC_2H_4NH_3I$). The resulting film was then immersed into an isopropanol: toluene mixed solution containing methylammonium iodide for different dipping duration (1–5 min) to convert it into higher dimensionality ($1 < n < \infty$). In this case, the 2D/3D ratio could be tuned by controlling the immersion time, and thus the optoelectronic properties, as well as the stability of mixed dimensional films. For the optimized films, they achieved the best PCE over 9%.[50]

The 2D-3D mixed perovskite approach has also been investigated in lead-free perovskite solar cells that are environmental more friendly but currently with low efficiency.[74-76] Recently, Loi and co-workers pushed the record PCE of Sn-based perovskite solar cells to 9% by adding a very small amount (8 mol%) of 2D layered tin perovskite into 3D tin perovskite. The 2D tin perovskite functioned as a seed layer to grow large and highly oriented 3D $FASnI_3$ grains. Moreover, 2D perovskite was also reported to fuse the $FASnI_3$ grains together and blurs the grain boundaries, which could reduce the possibility of forming Sn vacancies and Sn^{4+}. In common with Etgar's result,[69] the devices with mixed 2D/3D tin perovskites showed a higher V_{oc} of 0.52 V than that with only 3D tin perovskite (V_{oc} of 0.45 V). Also, after 76 h exposure to air, the device based on pure 3D perovskite completely failed, whereas the device based on 2D/3D mixture retained 59% of its original PCE.[71]

Therefore, although the 2D components typically only account for a small fraction in the 2D/3D mixed perovskite films, the incorporation of a suitable amount of 2D components could significantly improve the performance of perovskite solar cells, where 2D component acts as a functional barrier to enhance the crystal growth orientation and prevent ambient erosion.

2.3 2D layered perovskites as interface engineering layer (protection layer)

There is always a trade-off between efficiency and stability when 2D perovskites are used as an absorber in the solar cells. However, the natural moisture resistance of 2D perovskites attracts people's attention to their potential as interfacial materials.

Li and co-workers invented a universal fabrication approach for stable and efficient $MAPbX_3$ perovskite solar cells by using in-situ formed 2D perovskite as an interfacial layer. The insertion of the branched polyethylenimine hydriodide (PEI·HI) on top of the hole transporting layer (PEDOT:PSS) helped form thin $(PEI)_2PbI_4$ layer during deposition of $MAPbX_3$ perovskites (**Figure 8**a). The $(PEI)_2PbI_4$ layer served as a multifunctional interface to enhance the photovoltaic performance in three aspects: 1) control over the morphology and grain growth of 3D perovskite films on it; 2) facilitate hole extraction from perovskite into hole transport layer by energy level alignment (Figure 8b); 3) improve moisture resistance with $(PEI)_2PbI_4$ at interface. As a result, they demonstrated devices with PCEs over 16% and 13.8% on the rigid and flexible substrates respectively, as well as the enhanced moisture stability (Figure 8c-e).[77]

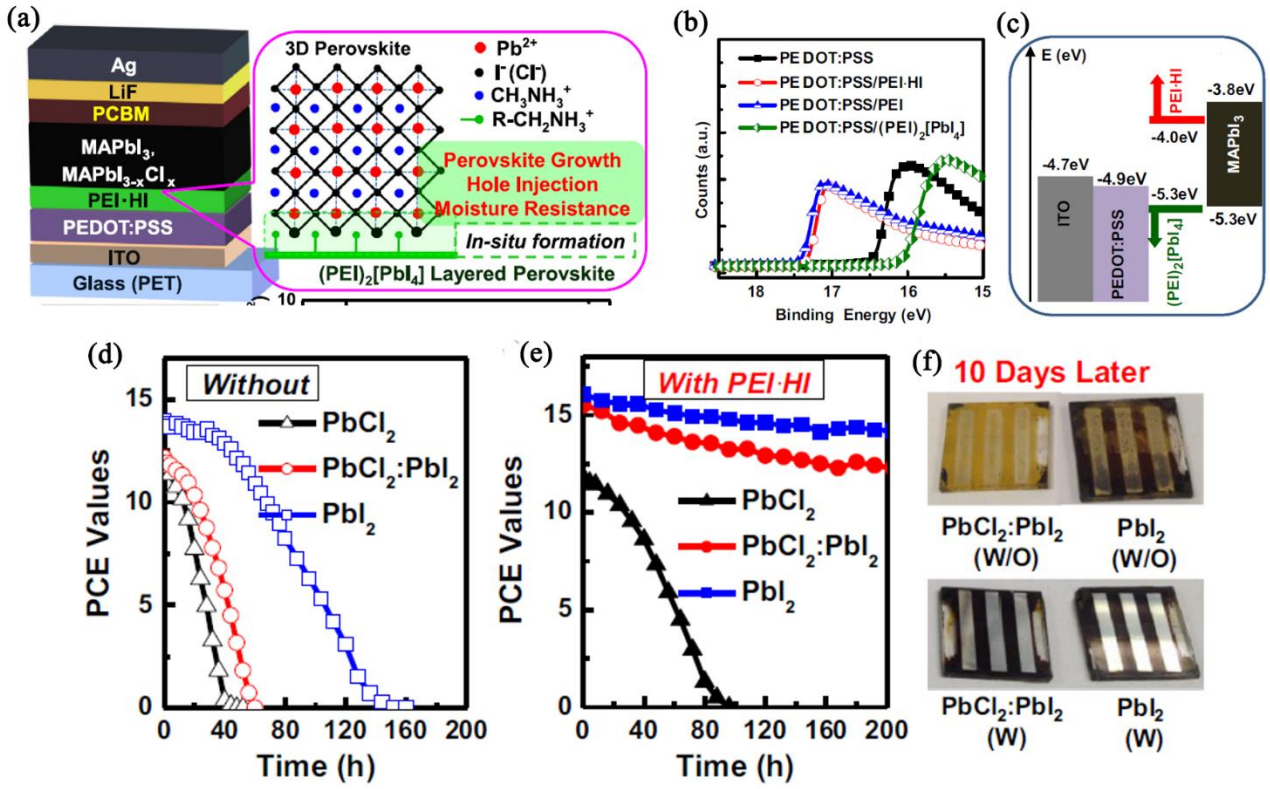

Figure 8. a) Schematic diagram of in-situ-generated layered perovskite $(PEI)_2[PbI_4]$. b) Work function measured from cut off obtained via UPS for PEDOT:PSS samples, with (PEI,PEI·HI or $(PEI)_2[PbI_4]$) and without modification. c) Schematic of the energy levels of each layer. Stability of perovskite photovoltaic devices without (d) and with (e) PEI·HI layer fabricated from different precursor $PbCl_2$:MAI, PbI_2:$PbCl_2$:MAI and PbI_2:MAI. Measurements under AM1.5 solar continuous illumination. f) Images of $MAPbI_{3-x}Cl_x$ and $MAPbI_3$ films after exposure to humidity for 10 days without (w/o) and with (w) PEI·HI layer. Reproduced with permission from Ref. 77. Copyright 2015, Elsevier Ltd

Yang *et al.* fabricated similar 3D-2D ($MAPbI_3$-$PEA_2Pb_2I_4$) graded perovskite interface on the top of the bulk 3D perovskite layer. The deposition process was based on the solvent engineering method but with a key modification: PEAI/toluene solution was used for the solvent dripping process instead of pure toluene. The 3D-2D graded interface modified the interface energy level and led to devices with an ultrahigh V_{oc} of 1.17 V and a PCE of 19.89%. More importantly, the graded interface also served as a self-encapsulation layer, suppressing internal cross-layer ion diffusion, slowing down the decomposition and degradation of the active layer and metal electrode in ambient, etc.[70]

Similarly, Shi *et al.* demonstrated another approach to forming a cyclopropylammonium (CA) based 2D perovskite (CA_2PbI_4) interfacial layer to cover the 3D perovskite ($MAPbI_xCl_{3-x}$). In their case, an additional spin coating of cyclopropylammonium iodide (CAI) solution in IPA was done on top of annealed 3D perovskite film. The thickness of in-situ 2D perovskite layer was adjustable according to the CAI concentration in solution. The devices with the optimized 2D perovskite interface achieved comparable PCE of 13.86% as compared to those without such an interface layer. However, they showed enhanced ambient stability by maintaining 54% of the original efficiency after 220 h, whereas the 3D perovskite device lost all the efficiency within only 50 h.[53]

Besides ammonium salts with large cations, different types of amine have also been utilized to form 2D perovskite interface layers on 3D perovskites, with the same approach as Shi *et al.* For example, Wong *et al.* applied benzylamine (BA^*) solution on the top of 3D $FA_{0.15}Cs_{0.85}Pb(I_{0.73}Br_{0.27})_3$ lattice (**Figure 9**a), leading to the formation of 2D layered perovskite ($BA^*_2PbI_4$) at grain boundaries and also top surface.[55] The perovskite films with such post-deposition treatment can suppress the photoinduced phase separation and decomposition, which is known for the high bandgap hybrid halogen Br/I.[78] The photostability and thermal stability tests showed that, after an 8 h ageing, the untreated films already presented a distinct XRD signal of PbI_2 at $2\theta = 12.7°$, indicating decomposition of the film, and the main XRD peak at 20.20° split into two peaks indicating the phase segregation. In contrast, the BA^*-treated films showed no obvious decomposition as well as phase segregation (Figure 9b-e). In addition, their champion devices based on the BA^*-treated film exhibited a stabilized power output efficiency of 17.1% and a high V_{oc} of 1.24 V. It maintained 80% of their original PCEs after 40 d exposure in ambient air with a humidity of 65 ± 5% RH, whereas the untreated devices degraded rapidly after 2 weeks.[55] Zhao and co-workers also treated their 3D $FAPbI_3$ perovskite films with aniline, benzylamine, and phenethylamine to compare the effects of different amines. They found the benzylamine modified films showed much better moisture resistance as compared to the others, despite the similarity in their chemical structures. The benzylamine treated films remained unchanged after

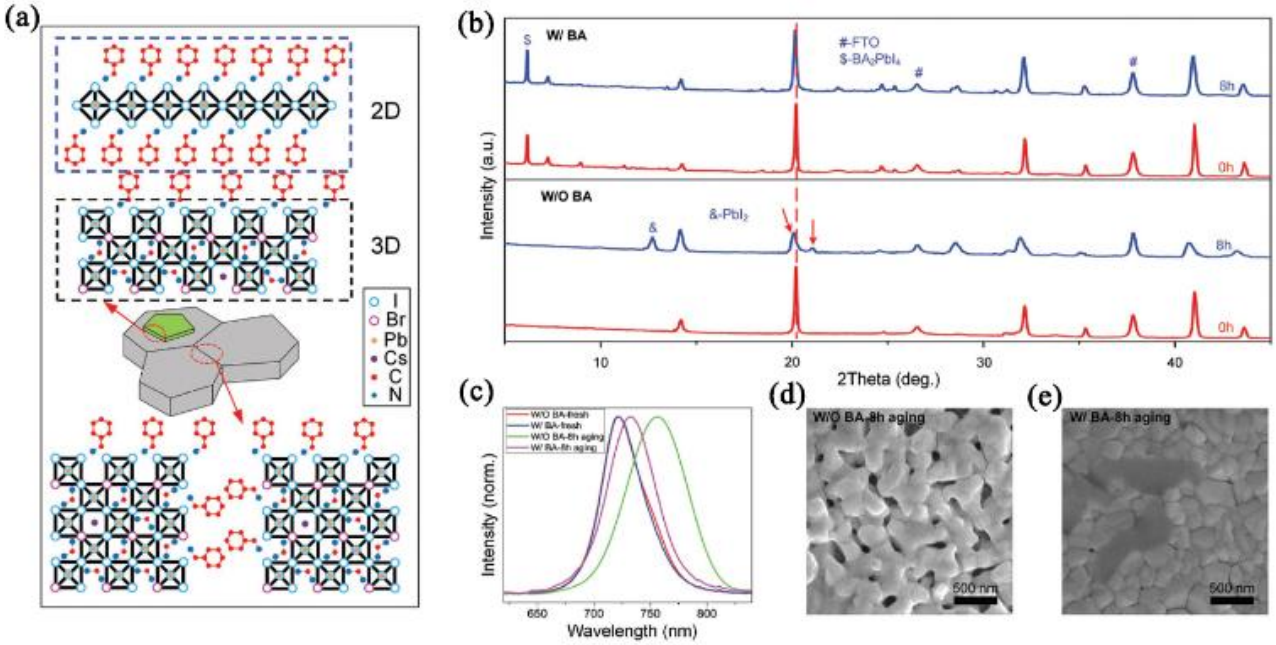

Figure 9. a) Schematic of the impact of BA* modification on the $Cs_{0.15}FA_{0.85}Pb(I_{0.73}Br_{0.27})_3$ thin film, illustrating the surface and grain boundaries passivation and 2D $BA^*_2PbI_4$ formation. b) XRD patterns and c) PL spectra of the films W/O BA* and W/ BA* aged 0 and 8 h under a white LED light source with an intensity of 200 mW cm^{-2} at 85 °C. SEM images of the films d) W/O BA* and e) W/ BA*aged 8 h under a white LED light source with an intensity of 200 mW cm^{-2} at 85 °C. Reproduced with permission from Ref. 55. Copyright 2017, Wiley-VCH

exposure to air (50 ± 5 RH%) for > 2900 h, while the untreated films degraded completely within 90 h under the same storage conditions.[79] They explained this as a molecular passivation effect because of the existence of the hydrophobic aromatic group which prevent the water molecule diffusion. However, according to Wong's view, it might be attributed to the formation of a thin 2D perovskite at interfaces after benzylamine treatment.

Recently, one-year stable perovskite solar cells were reported by Nazeeruddin and co-workers.[52] An exceptional gradually-organized multi-dimensional interface was formed in their 2D/3D perovskite junction, resulting in devices with the best PCE of 11.2% and stability for >10,000 h with zero loss. Different from the work mentioned above, the 2D component was found to self-assemble between mental oxide layer and 3D perovskite bulk after spin coating the precursor solution containing a small amount (< 5% molar ratio) of aminovaleric acid iodide (AVAI). The favourable anchoring of the carboxylic acid group of the AVAI ligand triggered the self-assembly of the 2D perovskite phase onto the TiO_2 scaffold. Moreover, this interface also promoted the oriented growth of the bulk 3D perovskite phase. Therefore, this 2D/3D interface brings together the enhanced stability of 2D perovskite and excellent charge transport of the 3D ones.

Compared to the 2D/3D mixed perovskites as the light absorber, the introduction of 2D perovskite as interface layer seems to be simpler and more effective. Either the self-assembled or post-treated 2D perovskite mainly existed on the surface of the whole active layer, and thus could keep all the advantages of 3D perovskite. Besides, the structural similarity of 2D and 3D perovskites guarantee the well-matched interface between 2D and 3D layers. Therefore, the devices show relatively higher PCE with 2D perovskite as interfacial layer.

3. Challenge and outlook

In the past few years, we have seen encouraging progress in perovskite solar cells based on 2D perovskites, with many demonstrations of devices showing high efficiency and long stability. Nevertheless, the efficiency of the devices based on 2D perovskite with low n values is still a lot lagging behind the 3D counterparts. Considering the increase of the bandgap with the decrease of the perovskite dimension, this type of perovskites may not be ideal materials for single junction perovskite solar cells since they will show intrinsically lower efficiency than the 3D ones. But they can be good large bandgap candidates for the tandem solar cells, and can possibly provide both high efficiency and good stability. On the other hand, devices with the 2D/3D mixed perovskites have shown similar efficiency but enhanced ambient stability compared to the ones based on their corresponding 3D counterparts, making them promising materials for further development. The approach of introducing 2D perovskite as interface layer has shown some success, yet a full understanding of the roles of such layers and treatments that are more generic and less delicate is still required. In terms of Sn-based perovskites, lowering their dimension seems to be a good way to prevent them from oxidation, but the device performance still needs to be improved.

To look forward, it is still necessary to gain more knowledge on the formation mechanism of 2D layer perovskites. This will enable us to fabricate phase-pure and highly out-of-plane oriented 2D perovskites or to grow 2D perovskites in 3D perovskite matrix in a more controlled way. In addition, scalable deposition method should be demonstrated for 2D perovskites, since there

are no high-efficiency large area modules reported for these materials so far. As for stability, researchers mainly focus on the ambient stability of the 2D perovskites at this moment, but ambient stability can be readily solved by encapsulation, making it less important in real application. Therefore, more focus should be put on the intrinsic heat or light stability of the 2D perovskites, in order to prove they are essentially better than their 3D counterparts. With material engineering, a large variety of novel 2D perovskites can be fabricated, and it will be interesting to investigate their properties and performance in different aspects. Overall, this is an exciting field to research and we can expect a lot more stimulating progress in the near future, which may eventually bring perovskite solar cells to commercialization.

Conflicts of interest

There are no conflicts to declare.

Acknowledgements

This work was supported by the National Natural Science Foundation of China (Grant Nos. 51620105006, 61721005), the Major State Basic Research Development Program (2014CB643503), Zhejiang Province Science and Technology Key Plan (No. 2018C01047), International Science and Technology Cooperation Program of China (ISTCP) (Grant No. 2016YFE0102900), and Zhejiang Province Natural Science Foundation (Grant No. LR15E030001). Weiming Qiu would like to thank the financial support of postdoctoral grant from the Research Fund Flanders (FWO). J. Yan thanks China Scholarship Council (CSC) for financial support.

Notes and references

1 G. Xing, N. Mathews, S. Sun, S. S. Lim, Y. M. Lam, M. Gratzel, S. Mhaisalkar and T. C. Sum, *Science*, 2013, **342**, 344-347.
2 Q. Q. Lin, A. Armin, R. C. R. Nagiri, P. L. Burn and P. Meredith, *Nature Photonics*, 2015, **9**, 106-112.
3 A. Marchioro, J. Teuscher, D. Friedrich, M. Kunst, R. van de Krol, T. Moehl, M. Gratzel and J. E. Moser, *Nature Photonics*, 2014, **8**, 250-255.
4 L. Protesescu, S. Yakunin, M. I. Bodnarchuk, F. Krieg, R. Caputo, C. H. Hendon, R. X. Yang, A. Walsh and M. V. Kovalenko, *Nano Lett.*, 2015, **15**, 3692-3696.
5 A. Kojima, K. Teshima, Y. Shirai and T. Miyasaka, *J. Am. Chem. Soc.*, 2009, **131**, 6050-6051.
6 I. Chung, B. Lee, J. He, R. P. Chang and M. G. Kanatzidis, *Nature*, 2012, **485**, 486-489.
7 J. H. Heo, S. H. Im, J. H. Noh, T. N. Mandal, C. S. Lim, J. A. Chang, Y. H. Lee, H. J. Kim, A. Sarkar, M. K. Nazeeruddin, M. Gratzel and S. I. Seok, Nature Photonics, 2013, 7, 487-492.
8 N. J. Jeon, J. H. Noh, Y. C. Kim, W. S. Yang, S. Ryu and S. I. Seok, *Nat Mater*, 2014, **13**, 897-903.
9 W. S. Yang, J. H. Noh, N. J. Jeon, Y. C. Kim, S. Ryu, J. Seo and S. I. Seok, *Science*, 2015, **348**, 1234-1237.
10 M. Saliba, T. Matsui, K. Domanski, J. Y. Seo, A. Ummadisingu, S. M. Zakeeruddin, J. P. Correa-Baena, W. R. Tress, A. Abate, A. Hagfeldt and M. Gratzel, *Science*, 2016, **354**, 206-209.
11 W. S. Yang, B. W. Park, E. H. Jung, N. J. Jeon, Y. C. Kim, D. U. Lee, S. S. Shin, J. Seo, E. K. Kim, J. H. Noh and S. I. Seok, *Science*, 2017, **356**, 1376-1379.
12 N. J. Jeon, J. H. Noh, W. S. Yang, Y. C. Kim, S. Ryu, J. Seo and S. I. Seok, *Nature*, 2015, **517**, 476-480.
13 M. Jaysankar, W. M. Qiu, M. van Eerden, T. Aernouts, R. Gehlhaar, M. Debucquoy, U. W. Paetzold and J. Poortmans, *Adv. Energy Mater.*, 2017, **7**, 1602807.
14 W. Qiu, T. Merckx, M. Jaysankar, C. M. de la Huerta, L. Rakocevic, W. Zhang, U. W. Paetzold, R. Gehlhaar, L. Froyen, J. Poortmans, D. Cheyns, H. J. Snaith and P. Heremans, *Energy. Environ. Sci.*, 2016, **9**, 484-489.
15 W. M. Qiu, A. Ray, M. Jaysankar, T. Merckx, J. P. Bastos, D. Cheyns, R. Gehlhaar, J. Poortmans and P. Heremans, *Adv. Funct. Mater.*, 2017, **27**, 1700920.
16 T. Leijtens, G. E. Eperon, S. Pathak, A. Abate, M. M. Lee and H. J. Snaith, *Nat. Commun.*, 2013, **4**, 2885.
17 N. G. Park, M. Gratzel, T. Miyasaka, K. Zhu and K. Emery, *Nature Energy*, 2016, 1, 16152.
18 B. Yang, O. Dyck, W. Ming, M. H. Du, S. Das, C. M. Rouleau, G. Duscher, D. B. Geohegan and K. Xiao, *ACS Appl. Mater. Interfaces*, 2016, **8**, 32333-32340.
19 M. Saliba, T. Matsui, J. Y. Seo, K. Domanski, J. P. Correa-Baena, M. K. Nazeeruddin, S. M. Zakeeruddin, W. Tress, A. Abate, A. Hagfeldt and M. Gratzel, *Energy. Environ. Sci.*, 2016, **9**, 1989-1997.
20 S. Yang, W. Liu, L. Zuo, X. Zhang, T. Ye, J. Chen, C. Z. Li, G. Wu and H. Chen, *J. Mater. Chem. A*, 2016, **4**, 9430-9436.
21 F. Li, H. Wang, D. Kufer, L. Liang, W. Yu, E. Alarousu, C. Ma, Y. Li, Z. Liu, C. Liu, N. Wei, F. Wang, L. Chen, O. F. Mohammed, A. Fratalocchi, X. Liu, G. Konstantatos and T. Wu, *Adv. Mater.*, 2017, **29**, 1602432.
22 H. Chen, W. Fu, C. Huang, Z. Zhang, S. Li, F. Ding, M. Shi, C. Z. Li, A. K. Y. Jen and H. Chen, *Adv. Energy Mater.*, 2017, **7**, 1700012.
23 C. Huang, W. Fu, C. Z. Li, Z. Zhang, W. Qiu, M. Shi, P. Heremans, A. K. Jen and H. Chen, *J. Am. Chem. Soc.*, 2016, **138**, 2528-2531.
24 L. Zuo, Z. Gu, T. Ye, W. Fu, G. Wu, H. Li and H. Chen, *J. Am. Chem. Soc.*, 2015, **137**, 2674-2679.
25 W. Qiu, J. P. Bastos, S. Dasgupta, T. Merckx, I. Cardinaletti, M. V. C. Jenart, C. B. Nielsen, R. Gehlhaar, J. Poortmans, P. Heremans, I. McCulloch and D. Cheyns, *J. Mater. Chem. A*, 2017, **5**, 2466-2472.
26 W. M. Qiu, M. Buffiere, G. Brammertz, U. W. Paetzold, L. Froyen, P. Heremans and D. Cheyns, *Org. Electron.*, 2015, **26**, 30-35.
27 Q. Dong, F. Liu, M. K. Wong, H. W. Tam, A. B. Djurisic, A. Ng, C. Surya, W. K. Chan and A. M. Ng, *ChemSusChem*, 2016, **9**, 2597-2603.
28 K. O. Brinkmann, J. Zhao, N. Pourdavoud, T. Becker, T. Hu, S. Olthof, K. Meerholz, L. Hoffmann, T. Gahlmann, R. Heiderhoff, M. F. Oszajca, N. A. Luechinger, D. Rogalla, Y. Chen, B. Cheng and T. Riedl, *Nat. Commun.*, 2017, **8**, 13938.
29 D. Koushik, W. J. H. Verhees, Y. H. Kuang, S. Veenstra, D. Zhang, M. A. Verheijen, M. Creatore and R. E. I. Schropp, *Energy. Environ. Sci.*, 2017, **10**, 91-100.
30 I. C. Smith, E. T. Hoke, D. Solis-Ibarra, M. D. McGehee and H. I. Karunadasa, *Angew. Chem. Int. Ed. Engl.*, 2014, **53**, 11232-11235.
31 D. H. Cao, C. C. Stoumpos, O. K. Farha, J. T. Hupp and M. G. Kanatzidis, *J. Am. Chem. Soc.*, 2015, **137**, 7843-7850.
32 X. Zhang, X. D. Ren, B. Liu, R. Munir, X. J. Zhu, D. Yang, J. B. Li, Y. C. Liu, D. M. Smilgies, R. P. Li, Z. Yang, T. Q. Niu, X. L. Wang, A. Amassian, K. Zhao and S. Z. F. Liu, *Energy. Environ. Sci.*, 2017, **10**, 2095-2102.

33 Y. Yamada, T. Nakamura, M. Endo, A. Wakamiya and Y. Kanemitsu, *J. Am. Chem. Soc.*, 2014, **136**, 11610-11613.
34 X. Zhang, G. Wu, S. Yang, W. Fu, Z. Zhang, C. Chen, W. Liu, J. Yan, W. Yang and H. Chen, *Small*, 2017, **13**, 1700611.
35 S. N. Ruddlesden and P. Popper, *Acta Crystallogr.*, 1957, **10**, 538-540.
36 D. B. Mitzi, *J. Mater. Chem.*, 2004, **14**, 2355-2365.
37 Z. N. Song, A. Abate, S. C. Watthage, G. K. Liyanage, A. B. Phillips, U. Steiner, M. Graetzel and M. J. Heben, *Adv. Energy Mater.*, 2016, **6**, 1600846.
38 X. Hong, T. Ishihara and A. V. Nurmikko, *Physical Review B*, 1992, **45**, 6961-6964.
39 Z. Guo, X. Wu, T. Zhu, X. Zhu and L. Huang, *ACS Nano*, 2016, **10**, 9992-9998.
40 R. L. Milot, R. J. Sutton, G. E. Eperon, A. A. Haghighirad, J. Martinez Hardigree, L. Miranda, H. J. Snaith, M. B. Johnston and L. M. Herz, *Nano Lett.*, 2016, **16**, 7001-7007.
41 J. Liu, J. Leng, K. Wu, J. Zhang and S. Jin, *J. Am. Chem. Soc.*, 2017, **139**, 1432-1435.
42 N. Wang, L. Cheng, R. Ge, S. Zhang, Y. Miao, W. Zou, C. Yi, Y. Sun, Y. Cao, R. Yang, Y. Wei, Q. Guo, Y. Ke, M. Yu, Y. Jin, Y. Liu, Q. Ding, D. Di, L. Yang, G. Xing, H. Tian, C. Jin, F. Gao, R. H. Friend, J. Wang and W. Huang, *Nat. Photon.*, 2016, **10**, 699-704.
43 H. Tsai, W. Nie, J. C. Blancon, C. C. Stoumpos, C. M. M. Soe, J. Yoo, J. Crochet, S. Tretiak, J. Even, A. Sadhanala, G. Azzellino, R. Brenes, P. M. Ajayan, V. Bulovic, S. D. Stranks, R. H. Friend, M. G. Kanatzidis and A. D. Mohite, *Adv. Mater.*, 2018, DOI: 10.1002/adma.201704217.
44 M. Yuan, L. N. Quan, R. Comin, G. Walters, R. Sabatini, O. Voznyy, S. Hoogland, Y. Zhao, E. M. Beauregard, P. Kanjanaboos, Z. Lu, D. H. Kim and E. H. Sargent, *Nat. Nanotechnol.*, 2016, **11**, 872-877.
45 J. Cho, Y. H. Choi, T. E. O'Loughlin, L. De Jesus and S. Banerjee, *Chem. Mater.*, 2016, **28**, 6909-6916.
46 T. Zhang, M. I. Dar, G. Li, F. Xu, N. Guo, M. Gratzel and Y. Zhao, *Sci. Adv.*, 2017, **3**, e1700841.
47 L. N. Quan, M. Yuan, R. Comin, O. Voznyy, E. M. Beauregard, S. Hoogland, A. Buin, A. R. Kirmani, K. Zhao, A. Amassian, D. H. Kim and E. H. Sargent, *J. Am. Chem. Soc.*, 2016, **138**, 2649-2655.
48 Y. Lin, Y. Bai, Y. Fang, Z. Chen, S. Yang, X. Zheng, S. Tang, Y. Liu, J. Zhao and J. Huang, *J. Phys. Chem. Lett.*, 2018, DOI: 10.1021/acs.jpclett.7b02679, 654-658.
49 Y. N. Chen, Y. Sun, J. J. Peng, W. Zhang, X. J. Su, K. B. Zheng, T. Pullerits and Z. Q. Liang, *Adv. Energy Mater.*, 2017, **7**, 1700162.
50 T. M. Koh, V. Shanmugam, J. Schlipf, L. Oesinghaus, P. Muller-Buschbaum, N. Ramakrishnan, V. Swamy, N. Mathews, P. P. Boix and S. G. Mhaisalkar, *Adv Mater*, 2016, **28**, 3653-3661.
51 J. Chen, J.-Y. Seo and N.-G. Park, *Adv. Energy Mater.*, 2018, 1702714.
52 G. Grancini, C. Roldan-Carmona, I. Zimmermann, E. Mosconi, X. Lee, D. Martineau, S. Narbey, F. Oswald, F. De Angelis, M. Graetzel and M. K. Nazeeruddin, *Nat. Commun.*, 2017, **8**, 15684.
53 C. Ma, C. Leng, Y. Ji, X. Wei, K. Sun, L. Tang, J. Yang, W. Luo, C. Li, Y. Deng, S. Feng, J. Shen, S. Lu, C. Du and H. Shi, *Nanoscale*, 2016, **8**, 18309-18314.
54 K. Yao, X. F. Wang, Y. X. Xu and F. Li, *Nano Energy*, 2015, **18**, 165-175.
55 Y. Zhou, F. Wang, Y. Cao, J. P. Wang, H. H. Fang, M. A. Loi, N. Zhao and C. P. Wong, *Adv. Energy Mater.*, 2017, **7**, 1701048.
56 B. Cohen, M. Wierzbowska and L. Etgar, *Sustainable Energy & Fuels*, 2017, **1**, 1935-1943.
57 T. M. Koh, V. Shanmugam, X. Guo, S. S. Lim, O. Filonik, E. M. Herzig, P. Müller-Buschbaum, V. Swamy, S. T. Chien, S. G. Mhaisalkar and N. Mathews, *J. Mater. Chem. A*, 2018, **6**, 2122-2128.
58 Y. Lin, Y. Bai, Y. J. Fang, Q. Wang, Y. H. Deng and J. S. Huang, *Acs Energy Letters*, 2017, **2**, 1571-1572.
59 J. C. Blancon, H. Tsai, W. Nie, C. C. Stoumpos, L. Pedesseau, C. Katan, M. Kepenekian, C. M. Soe, K. Appavoo, M. Y. Sfeir, S. Tretiak, P. M. Ajayan, M. G. Kanatzidis, J. Even, J. J. Crochet and A. D. Mohite, *Science*, 2017, **355**, 1288-1292.
60 X. Zhang, G. Wu, W. Fu, M. Qin, W. Yang, J. Yan, Z. Zhang, X. Lu and H. Chen, *Adv. Energy Mater.*, 2018, 1702498.
61 H. Tsai, W. Nie, J.-C. Blancon, C. C. Stoumpos, R. Asadpour, B. Harutyunyan, A. J. Neukirch, R. Verduzco, J. J. Crochet, S. Tretiak, L. Pedesseau, J. Even, M. A. Alam, G. Gupta, J. Lou, P. M. Ajayan, M. J. Bedzyk, M. G. Kanatzidis and A. D. Mohite, *Nature*, 2016, **536**, 312-316.
62 J. F. Liao, H. S. Rao, B. X. Chen, D. B. Kuang and C. Y. Su, *J. Mater. Chem. A*, 2017, **5**, 2066-2072.
63 D. H. Cao, C. C. Stoumpos, T. Yokoyama, J. L. Logsdon, T.-B. Song, O. K. Farha, M. R. Wasielewski, J. T. Hupp and M. G. Kanatzidis, *ACS Energy Letters*, 2017, **2**, 982-990.
64 C. M. M. Soe, W. Nie, C. C. Stoumpos, H. Tsai, J.-C. Blancon, F. Liu, J. Even, T. J. Marks, A. D. Mohite and M. G. Kanatzidis, *Adv. Energy Mater.*, 2018, **8**, 1700979.
65 J. Yan, W. Fu, X. Zhang, J. Chen, W. Yang, W. Qiu, G. Wu, F. Liu, P. Heremans and H. Chen, *Materials Chemistry Frontiers*, 2018, **2**, 121-128.
66 N. Zhou, Y. Shen, L. Li, S. Tan, N. Liu, G. Zheng, Q. Chen and H. Zhou, *J. Am. Chem. Soc.*, 2018, **140**, 459-465.
67 Z. Wang, Q. Lin, F. P. Chmiel, N. Sakai, L. M. Herz and H. J. Snaith, *Nature Energy*, 2017, **6**, 17135.
68 N. Li, Z. Zhu, C.-C. Chueh, H. Liu, B. Peng, A. Petrone, X. Li, L. Wang and A. K. Y. Jen, *Adv. Energy Mater.*, 2017, **7**, 1601307.
69 B.-E. Cohen, M. Wierzbowska and L. Etgar, *Adv. Funct. Mater.*, 2017, **27**, 1604733.
70 Y. Bai, S. Xiao, C. Hu, T. Zhang, X. Y. Meng, H. Lin, Y. L. Yang and S. H. Yang, *Adv. Energy Mater.*, 2017, **7**, 1701038.
71 S. Shao, J. Liu, G. Portale, H.-H. Fang, G. R. Blake, G. H. ten Brink, L. J. A. Koster and M. A. Loi, *Adv. Energy Mater.*, 2017, 1702019.
72 W. Fu, J. Yan, Z. Zhang, T. Ye, Y. Liu, J. Wu, J. Yao, C.-Z. Li, H. Li and H. Chen, *Solar Energy Materials and Solar Cells*, 2016, **155**, 331-340.
73 Y. Liao, H. Liu, W. Zhou, D. Yang, Y. Shang, Z. Shi, B. Li, X. Jiang, L. Zhang, L. N. Quan, R. Quintero-Bermudez, B. R. Sutherland, Q. Mi, E. H. Sargent and Z. Ning, *J. Am. Chem. Soc.*, 2017, **139**, 6693-6699.
74 C. M. Tsai, N. Mohanta, C. Y. Wang, Y. P. Lin, Y. W. Yang, C. L. Wang, C. H. Hung and E. W. Diau, *Angew Chem Int Ed Engl*, 2017, **56**, 13819-13823.
75 J. Xi, Z. Wu, B. Jiao, H. Dong, C. Ran, C. Piao, T. Lei, T. B. Song, W. Ke, T. Yokoyama, X. Hou and M. G. Kanatzidis, *Adv. Mater.*, 2017, **29**, 1606964.
76 X. Zhang, G. Wu, Z. Gu, B. Guo, W. Liu, S. Yang, T. Ye, C. Chen, W. Tu and H. Chen, *Nano Research*, 2016, **9**, 2921-2930.
77 K. Yao, X. Wang, Y.-x. Xu and F. Li, *Nano Energy*, 2015, **18**, 165-175.
78 E. T. Hoke, D. J. Slotcavage, E. R. Dohner, A. R. Bowring, H. I. Karunadasa and M. D. McGehee, *Chem. Sci.*, 2015, **6**, 613-617.
79 F. Wang, W. Geng, Y. Zhou, H. H. Fang, C. J. Tong, M. A. Loi, L. M. Liu and N. Zhao, *Adv. Mater.*, 2016, **28**, 9986-9992.